Oscillators and Amplifiers in Integrated *E*-Plane Technique

WOLFGANG J. R. HOEFER, SENIOR MEMBER, IEEE

(Invited Paper)

Abstract —**This paper presents an overview of solid-state oscillators and amplifiers realized in *E*-plane technology. The circuit topology, basic design procedures, and performance characteristics are described and compared. The paper surveys Gunn oscillators, IMPATT oscillators, transistor oscillators, injection-locked Gunn oscillators, and transistor amplifiers. Gunn and transistor oscillators have been realized successfully for frequencies from 10 to 110 GHz, thus covering almost the entire frequency range suitable for *E*-plane technology. IMPATT oscillators are difficult to design and to reproduce in quasi-planar form because of the high impedance ratio that must be overcome by the circuit. *E*-plane FET amplifiers have been built for frequencies up to 60 GHz.**

I. Introduction

THE DEVELOPMENT of *E*-plane components has significantly contributed to the proliferation of millimeter-wave systems for communications, radar, radiometry, and remote sensing. *E*-plane technology offers a unique combination of advantages, including a high performance/cost ratio, design flexibility, potential for circuit integration, and compatibility with solid-state devices and waveguide. Its principal range of application covers frequencies between 10 and 100 GHz, with some realizations reaching 170 GHz.

Components for power generation and amplification are crucial for realizing integrated *E*-plane systems such as the radar transceiver front end shown in Fig. 1. This circuit combines, on a single substrate, a balanced mixer with its local oscillator, several switches, and the radar pulse oscillator.

This paper presents a survey of the various *E*-plane oscillators and amplifiers that have been realized to date. The most important design considerations and typical performance characteristics are summarized. For more detailed information on the individual realizations, the reader is referred to the original papers.

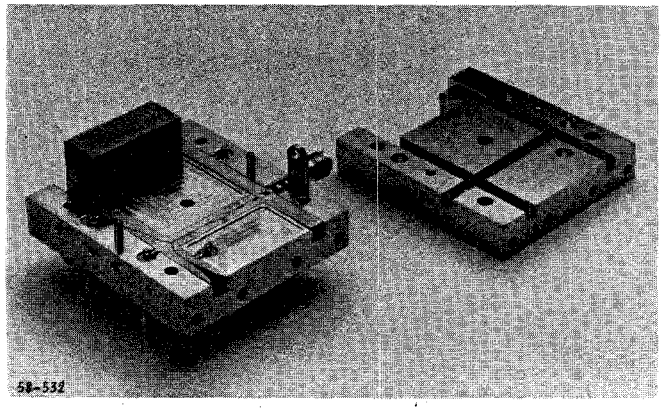

Fig. 1. Integrated *Ka*-band pulse radar front end in *E*-plane technique (courtesy of AEG AG., Ulm).

II. Gunn Diode Oscillators

A variety of Gunn diode oscillators in *E*-plane configuration have been built for frequencies between roughly 10 and 100 GHz, covering nearly the complete range suitable for *E*-plane technology. Their main differences reside in the construction and topology of their passive circuit, which has the following functions:

i) to bias the diode(s) and provide adequate RF/dc decoupling,
ii) to determine the oscillation frequency without ambiguity,

Manuscript received January 25, 1988; revised July 26, 1988.
The author is with the Laboratory for Electromagnetics and Microwaves, Department of Electrical Engineering, University of Ottawa, Ottawa, Ont., Canada K1N 6N5.
IEEE Log Number 8824992.

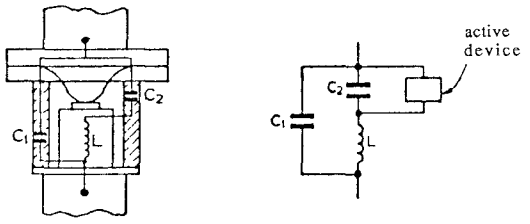

TYPICAL PACKAGE REACTANCE PARAMETERS

10 GHz Device [S4]: $C_1 = 0.10$ pF, $C_2 = 0.12$ pF, $L = 0.65$ nH

60 GHz Device: $C_1 = 0.09$ pF, $C_2 = 0.28$ pF, $L = 0.08$ nH

Fig. 2. Parasitic reactances of a Gunn-diode package (after Owens and Cawsey [1]).

iii) to provide optimum impedance transformation between the active element and the load,
iv) to provide adequate heatsinking.

The circuit type is selected according to the following criteria:

a) frequency of operation,
b) efficiency,
c) mechanical/electronic tunability,
d) active/passive stabilization.

All realizations described in this paper share important advantages: their design is very flexible owing to the planar nature of the circuitry. The active elements are easy to bias, and can be mounted in the walls of the waveguide enclosure for effective heatsinking. But most importantly, they can be integrated with other components to form complete subsystems, as in Fig. 1.

Due to the parasitic package reactances, the source impedance of Gunn diodes depends strongly on the operating frequency. A packaged device can be represented by the Pi equivalent circuit [1] shown in Fig. 2. At low frequencies, the real part of the source impedance Z_s of the packaged device is of the order of -10 to -30 Ω, while at frequencies above 40 GHz it reaches typically -100 Ω. However, the minimum practical characteristic impedance level of *E*-plane lines (with the exception of antipodal finline) is about 100 Ω. Thus, the impedance ratio to be overcome by the transformer network decreases with increasing frequency. Furthermore, fundamental-mode operation of GaAs Gunn devices is limited to frequencies below 70 GHz, and second-harmonic extraction must be used. Again, this requires completely different circuit topologies.

In the following, the principal Gunn oscillator types will be described, and their most important design and performance characteristics will be discussed.

A. Gunn Oscillators with Planar Post Mounts

In conventional waveguide Gunn oscillators, the source impedance of the diode is matched to the waveguide by a cylindrical inductive post and a backshort. Knoechel [2]

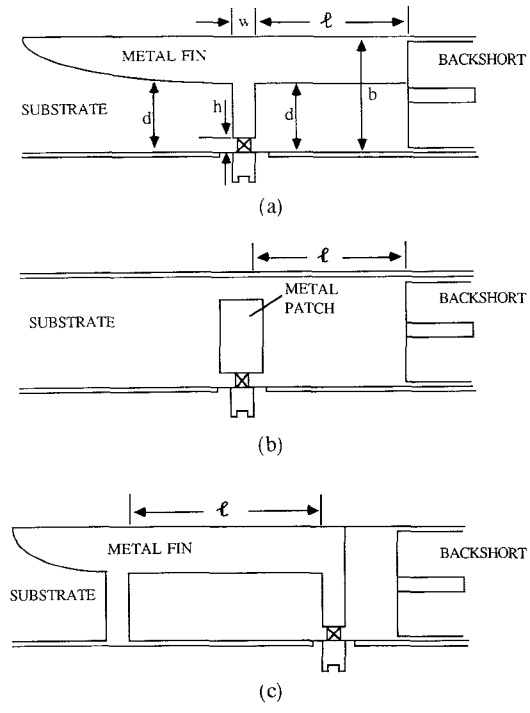

Fig. 3. Three Gunn-diode mounts proposed by Knoechel [2]. (a) Planar post mount. (b) Antenna mount. (c) Transmission cavity mount.

has conducted an extensive experimental study on quasi-planar versions of such oscillators. Fig. 3 shows his most successful topologies. Note that Knoechel experimented at frequencies around 15 GHz, where the source impedance of packaged devices is at least one order of magnitude lower than the characteristic impedance of *E*-plane lines (finlines). Indeed, the planar post configuration is well suited for lower frequencies since it can realize such large impedance transformer ratios. For maximum efficiency, Knoechel recommends that the gap width of the finline be chosen as large as possible, in which case the oscillator becomes effectively a waveguide component with a comparable performance.

Knoechel [2] has designed and optimized the oscillators in Fig. 3 experimentally around 15 GHz. He adjusted the dimensions of the circuits by observing on a network analyzer the driving impedance seen by the diode. However, El Hennawy and Schuenemann [3] and Zhang and Itoh [4] have published theoretical curves useful for the design of the planar post mount of Fig. 3(a). The data by El Hennawy and Schuenemann are for single-finned unilateral finlines with slot widths less than the waveguide height, while Zhang and Itoh have computed the equivalent network parameters for *E*-plane strips in slab-loaded waveguides. Even though the data are for *Ka*-band, they can be scaled for other waveguide bands.

Fig. 4(a) shows the equivalent circuit of the planar post mount of Fig. 3(a). It is assumed that only the dominant mode is propagating in the finline. All quantities are normalized to the characteristic impedance of the finline. (It is a single-finned unilateral line; its characteristic impedance is half the value of a square-section finline of

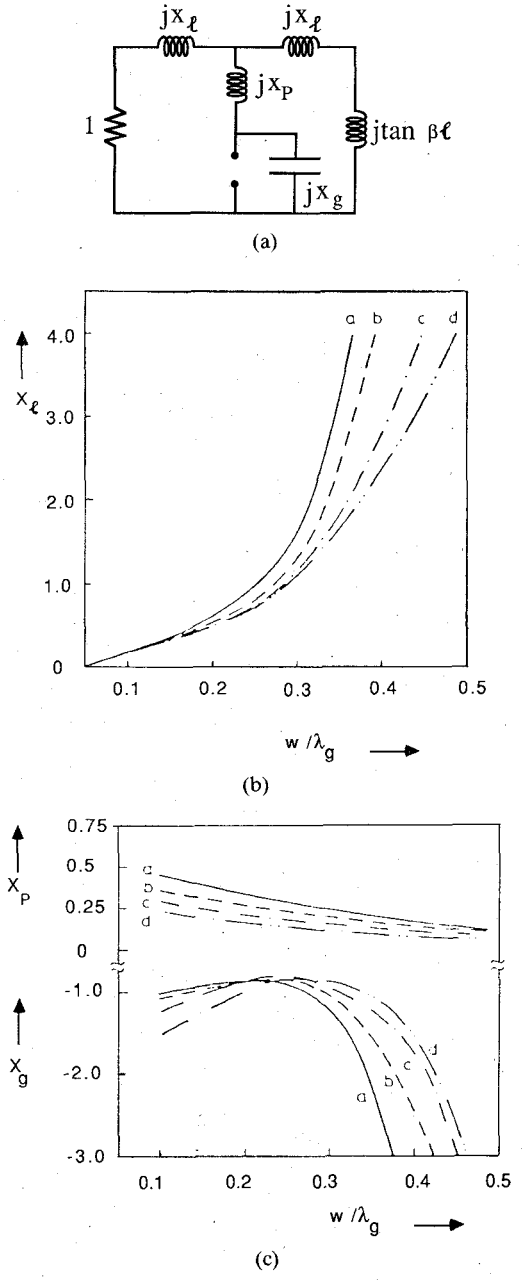

Fig. 4. (a) Equivalent circuit of the planar post mount in Fig. 3(a). (b) Normalized series reactance x_l of the post. (c) Normalized shunt inductance x_p and gap capacitance x_g of the post. (After El Hennawy and Schuenemann [3].) $f = 30$ GHz, $h = 1$ mm, $a = 7.112$ mm, $b = 3.556$ mm (WR-28), substrate thickness = 0.254 mm, $\epsilon_r = 2.2$, curve a: $d = 3.0$ mm, curve b: $d = 2.5$ mm, curve c: $d = 2.0$ mm, curve d: $d = 1.5$ mm.

slot width $2d$ and inner housing dimensions $a \times 2b$, while the guided wavelength λ_g is the same in both structures.) The quantities jx_l and jx_p represent the equivalent inductances of the planar post and are nearly equal to those of a transverse strip ($h = 0$); jx_g is the gap capacitance. The normalized load is unity, and the backshort adds a normalized inductance $j \tan \beta l$ in parallel.

The diagrams in Fig. 4(b) and (c), which are reproduced from [3], show these reactances versus the normalized width w/λ_g of the planar post for four different finline slot widths. Fig. 5 represents the gap impedance normal-

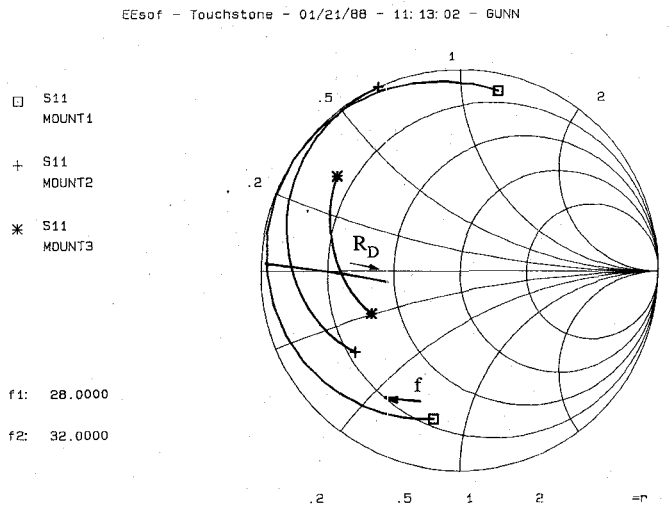

Fig. 5. Driving impedance of the planar post mount in Fig. 3(a), seen by the diode. $h = 1$ mm, $d = 3$ mm, $a = 7.112$ mm, $b = 3.556$ mm (WR-28), substrate thickness = 0.254 mm, $\epsilon_r = 2.2$. Mount 1: $w = 3.74$ mm; Mount 2: $w = 2.49$ mm; Mount 3: $w = 1.25$ mm.

ized to the finline impedance, as "seen" by the packaged diode, for three planar posts as a function of frequency. The backshort has been adjusted in such a way that in each case the gap impedance became real at 30 GHz. A typical device line is also shown in this diagram. Note that the operating value of the diode resistance R_d is determined by the width of the post, while the frequency of oscillation can be tuned with the backshort.

For each value of d there is an optimum post width yielding maximum Q. This maximum grows with increasing w. However, since the width of the post is usually determined by the impedance-matching condition, one additional degree of freedom is needed to optimize the Q factor of the oscillator. This can be accomplished by adding a transmission cavity between the oscillator and the load, as shown in Fig. 3(c).

The antenna mount in Fig. 3(b) has characteristics similar to those of the planar post mount. However, the biasing of the device requires the introduction of a wire into the waveguide, and care must be taken to avoid interference of this wire with the RF field. Such an antenna-mount oscillator has been incorporated into a *Ku*-band receiver front end by Begemann *et al.* [5]. Typical performance characteristics for a 15 GHz planar post oscillator by Knoechel [2] are shown in Fig. 6.

B. Gunn Oscillators with Resonator-Mounted Diodes

Hofmann *et al.* [6] have proposed a variety of *E*-plane oscillators in which the diode is mounted in the end wall of the waveguide housing and coupled directly to a resonant line section (Fig. 7). At the load end, the resonator is bounded by an inductive discontinuity in the form of a transverse metallic bridge (Fig. 7(a)), a transverse strip on the back side of the substrate (Fig. 7(b)), or, when the resonant line is a microstrip suspended in the *E* plane, a slot in the back metallization (Fig. 7(c)). In all three cases, the oscillator can be represented by the equivalent circuit

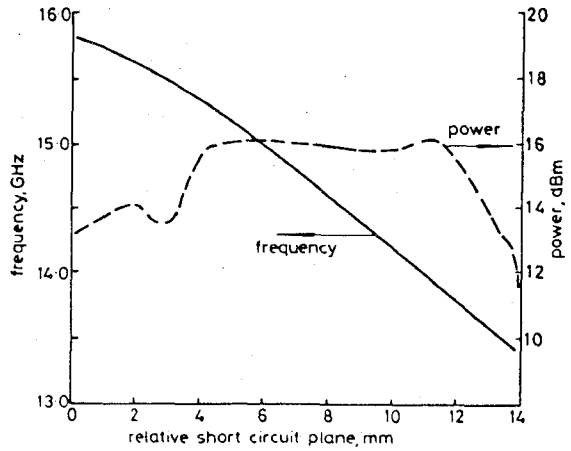

Fig. 6. Performance of the planar post mount oscillator (after Knoechel [2]).

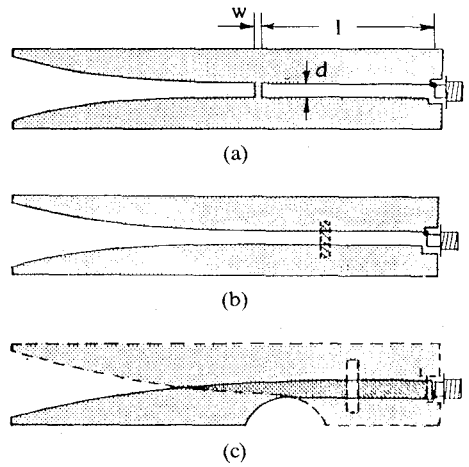

Fig. 7. Gunn oscillators with resonator-mounted diodes. (a) Finline resonator with transverse metallic bridge. (b) Finline resonator with backside strip. (c) Microstrip resonator with slot in the ground plane. (After Hofmann, Meinel, and Adelseck [6].)

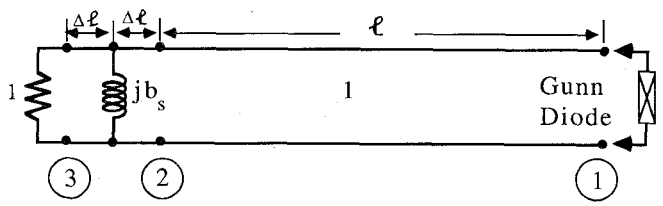

Fig. 8. Equivalent circuit of resonator-mounted diode oscillators in Fig. 7.

shown in Fig. 8. While the oscillation frequency is essentially determined by the electrical length of the resonant section, the impedance seen by the diode depends on the characteristic impedance of the line and the width, i.e., the inductance of the obstacle. Fig. 9 shows the impedance seen by the diode in the circuit of Fig. 7(a). The finline slot width d is 1 mm, and three different strips ($w = 1$, 2, and 3 mm) have been selected. The length l of the resonator has been adjusted such that the impedance seen by the diode is real at 30 GHz. The normalized susceptance and the electrical width of the inductive strip have been obtained from data published by Pic and Hoefer [7]. This type of

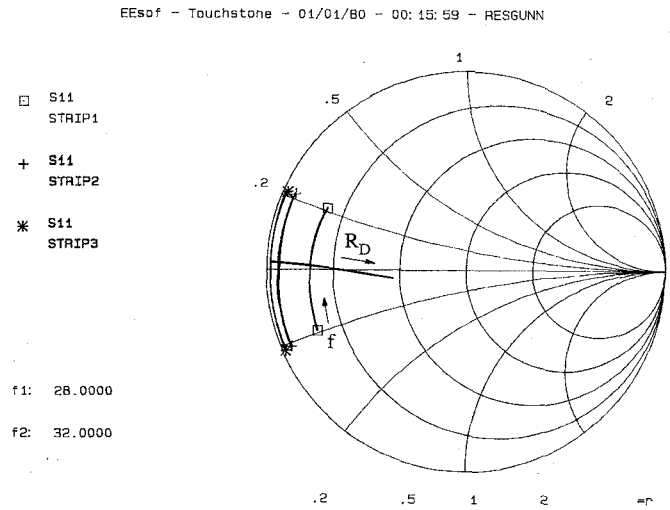

Fig. 9. Driving impedance of the oscillator in Fig. 7(a), seen by the diode. $d = 0.89$ mm, $a = 7.112$ mm, $b = 3.556$ mm (WR-28), substrate thickness = 0.254 mm, $\epsilon_r = 2.2$. Strip 1: $w = 0.1$ mm; Strip 2: $w = 0.5$ mm; Strip 3: $w = 1.0$ mm.

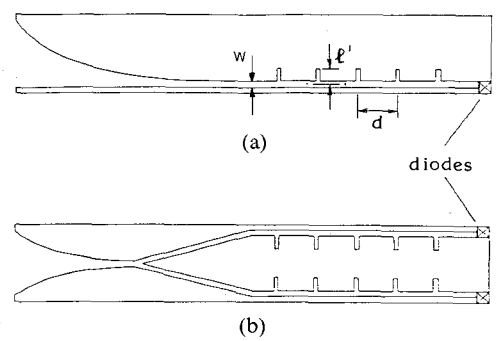

Fig. 10. Gunn oscillators with grating structures. (a) Layout for a single diode. (b) Layout for two diodes. (After Adelseck, Sicking, and Hofmann [11].)

oscillator does not possess a backshort for frequency tuning, and has a lower Q factor (typically around 60 in *Ka*-band) than the post-coupled versions discussed above, due to the increased losses in the finline resonator.

C. Gunn Oscillators with Grating Structures

This oscillator type has been proposed by Hofmann [8], who was inspired by earlier work by Itoh and Hsu [9] on optical grating structures. Fig. 10 shows two versions, one for a single diode and one for two diodes in a tandem configuration. The oscillator circuit consists of a single-ridged finline with a number of equally spaced series slots acting as a slow-wave structure.

Its characteristics can be computed approximately by assuming that the series stubs are slotlines with an effective length l',

$$l' = l + w/2 \tag{1}$$

where l is the physical length of the stubs, and w is the slot width of the unsymmetrical main line. This approximation is best when the series slots are much narrower than w. A more accurate model for series slots, which take into account the frequency-dependent parasitics at both

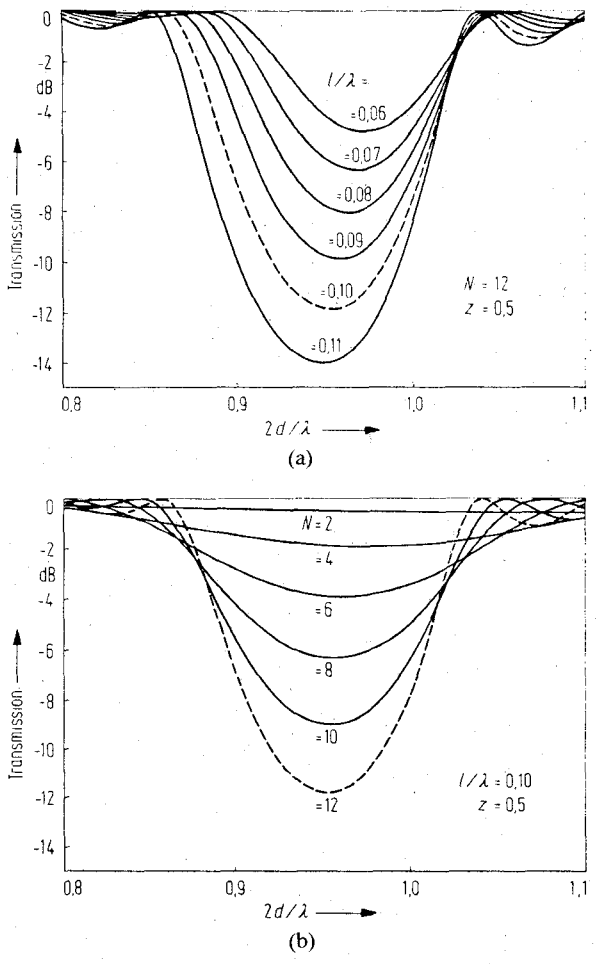

Fig. 11. Transmission characteristics of the grating structure in Fig. 10(a). (a) Grating structure with $N=12$ series stubs of normalized impedance $z=0.5$ for several stub lengths l/λ. (b) Grating structures with different numbers N of stubs with $z=0.5$ and $l/\lambda=0.1$. (After Adelseck, Sicking, and Hofmann [11].)

ends of the slots, has been developed by Burton and Hoefer [10]. The characteristics of the grating structure can thus be determined with good accuracy. Fig. 11 shows the transmission characteristics of the periodic structure for various slot lengths (Fig. 11(a)) and for different numbers of slots (Fig. 11(b)) as calculated by Adelseck *et al.* [11]. The oscillator operates in the first stopband of the structure. Fig. 12 shows the normalized impedance seen by the diode in Fig. 10(a), together with a field of device lines for a typical 35 GHz Gunn diode [11]. During the design procedure, the number, length, and spacing of the series slots are selected to realize a reflection coefficient of appropriate magnitude. Its phase is then determined by the proper distance between the diode and the nearest slot. Note that the frequency of oscillation is essentially governed by the spacing between the series slots, while the impedance is determined by the length of the slots.

Adelseck *et al.* [11] have given the following guidelines for the design of grating oscillators:

i) If the series slots are modeled according to (1) above, their width should be much smaller than that of the main slot for best design accuracy.

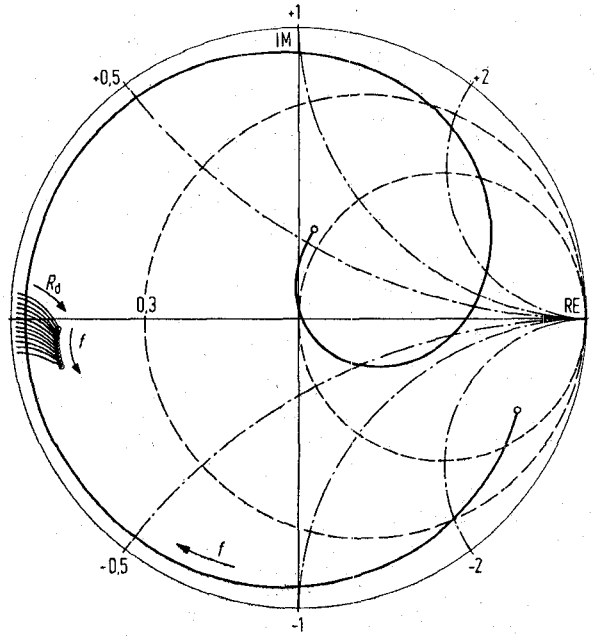

Fig. 12. Typical driving impedance of the grating structure in Fig. 10(a), seen by the diode (after Adelseck, Sicking, and Hofmann [11]).

ii) For best results, the number of slots should be between four and seven. With fewer than four slots, the stopband becomes too large, and for more than seven slots, the modeling accuracy becomes poor.

iii) The length of the slots should not be close to $\lambda/4$, since in that case the next stopband of the structure comes too close to the design frequency, which increases the risk of frequency jumping.

Typical performance characteristics for this oscillator type, as reported by Adelseck *et al.* [11], are as follows. *Ka*-band oscillators (26.5–40 GHz) delivered up to 135 mW with a single diode, and 260 mW with two diodes in a tandem configuration. They oscillated within 3 percent of the design frequency and could easily be tuned by placing a waveguide backshort behind the diode. Similar performance was achieved in the *V*-band (50–75 GHz). Typical Q factors were around 140, and the temperature stability was measured as $3\times10^{-5}/°\mathrm{K}$.

D. Direct-Mounted Gunn Oscillators

At frequencies above 40 GHz, the source impedance of packaged Gunn diodes approaches values of the order of typical line impedances, so that they can be mounted directly into a finline as shown in Fig. 13. Such oscillators have been built by Hofmann *et al.* [6] and Cohen and Meier [12]. No impedance transformer is necessary at these frequencies, and the backshort essentially adjusts the frequency with a minimal effect on the output power. Fig. 13 shows that the construction of such an oscillator is extremely simple. The diode is mounted in a copper heatsink at the bottom of the waveguide enclosure and is soldered either directly or bonded with a gold foil to the printed fin. The finline slot width is primarily determined by the height of the diode head. The serrations in Fig. 13(b)

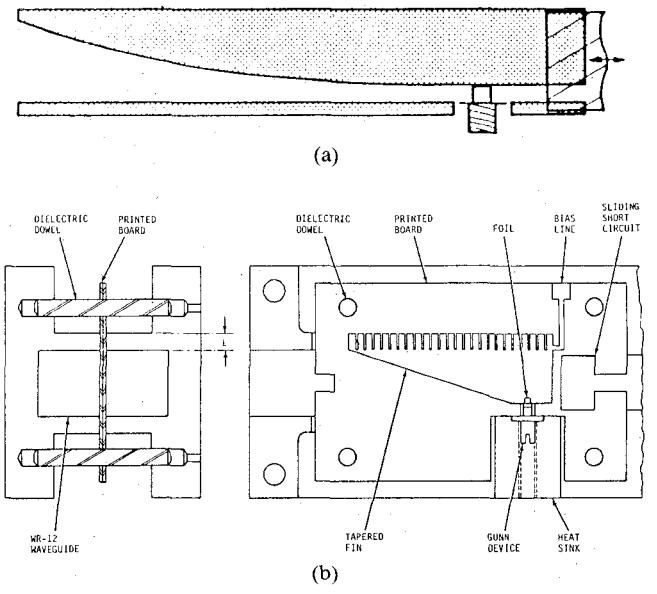

Fig. 13. Direct-mounted Gunn oscillators. (a) Oscillator by Hofmann, Meinel and Adelseck [6]. (b) Oscillator by Cohen and Meier [12].

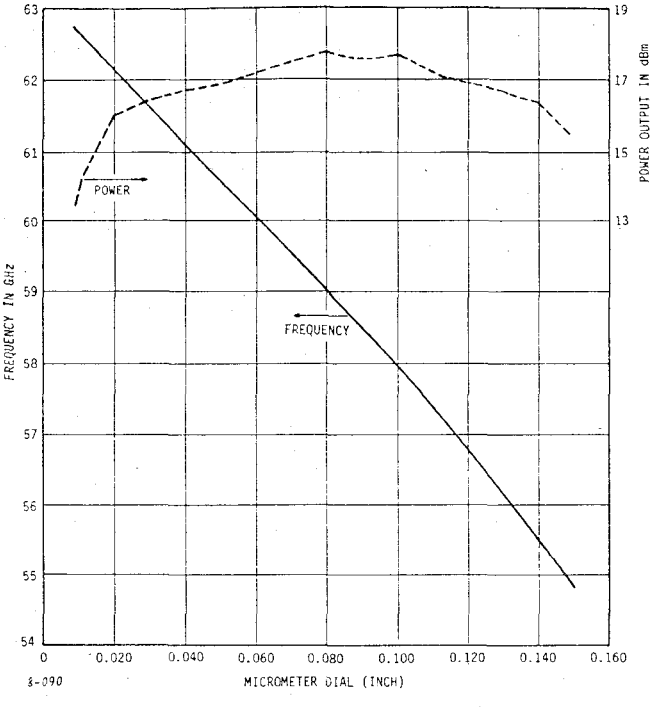

Fig. 14. Direct-mounted oscillator performance with GaAs Gunn diode (after Cohen and Meier [12]).

suppress longitudinal currents in the clamping region of the housing and act as a $\lambda/4$ choke. Hence, no special low pass is needed in the dc bias line. Typical performance characteristics obtained by Cohen and Meyer [12] with GaAs and InP Gunn diodes are shown in Figs. 14 and 15. These diagrams confirm that the backshort provides smooth frequency tunability without deterioration of the output power. Typically, power levels of 63 mW were achieved at 59 GHz with GaAs diodes, and 46 mW at 67 GHz with InP diodes.

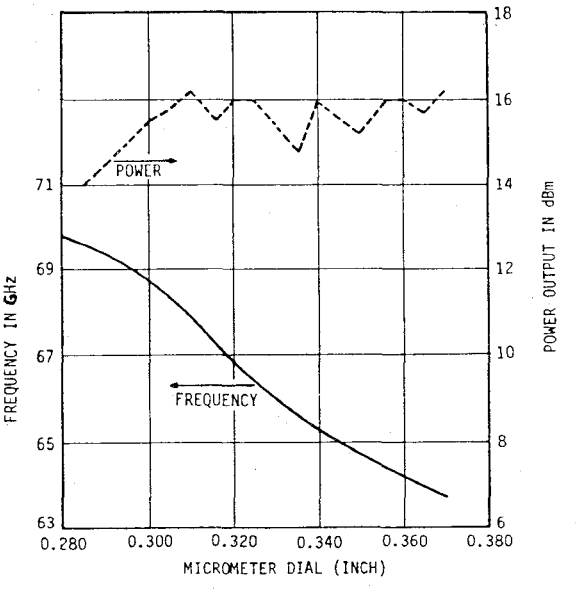

Fig. 15. Direct-mounted oscillator performance with InP Gunn diode (after Cohen and Meier [12]).

E. Second-Harmonic Gunn Oscillators

For frequencies above 65 GHz, second (or sometimes higher) harmonic extraction is commonly used. Such oscillators contain a resonant circuit for the fundamental frequency, but energy is extracted only at a higher harmonic frequency.

Cohen [13] has realized such an oscillator by placing a disk between the printed fin and the top of the Gunn diode package in Fig. 13(b). In combination with the diode reactances, the disk forms a resonant circuit at the fundamental, and matches the diode to the output waveguide at the second harmonic frequency. Output power of typically 5 mW was obtained in the 85 to 94 GHz range, and a value of up to 10 mW was achieved with selected diodes at 94 GHz. The mechanical tuning range was 2 GHz. Attempts to realize such oscillators entirely in quasi-planar technique have been less satisfactory. Fig. 16 shows two experimental 90 GHz second-harmonic Gunn oscillator circuits [14]. In Fig. 16(a), the diode is mounted in a finline resonator which can sustain both the fundamental and the second-harmonic frequency of the oscillator. While the fundamental oscillation cannot propagate in the adjacent regions, the harmonic oscillation is coupled to the output via a comb-shaped impedance transformer. Fig. 16(b) shows a planar version of Cohen's "cap" structure.

The performance of these oscillators was disappointing: only 20 to 150 μW could be extracted at frequencies between 73 and 110 GHz. This was attributed to the fact that the planar structures and the Gunn element could not be modeled with sufficient accuracy; nor could they be easily adjusted for optimum performance. Furthermore, since the source impedance at the second harmonic is of the order of 1 Ω, the required transformer ratio of 200 to 500 can only be realized with great difficulty and at the expense of very high losses. It was therefore concluded

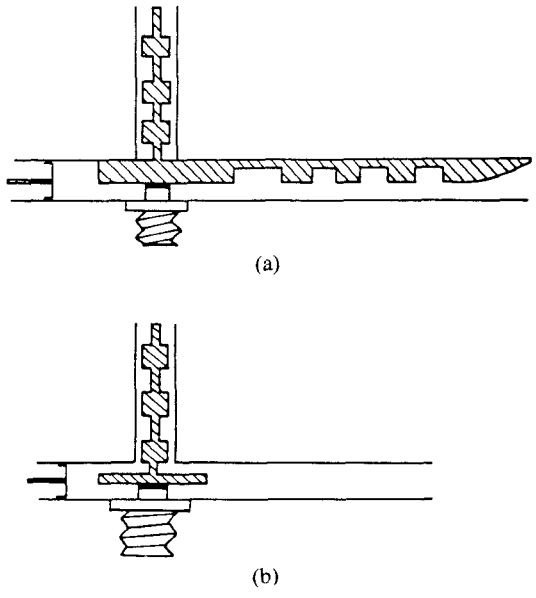

Fig. 16. Experimental second-harmonic Gunn oscillators in E-plane technique. (a) Circuit with finline resonator. (b) Circuit with planar "cap" resonator. (Courtesy of AEG AG, Ulm.)

that quasi-planar technology is not suitable for the realization of second-harmonic Gunn oscillators.

F. Varactor-Tuned Gunn Oscillators

Electronically tunable Gunn oscillators in E-plane technique have been described by Knoechel [2], Cohen [13], Erichsen *et al.* [15], and Solbach *et al.* [16]. The varactor-tuned oscillator discussed by Knoechel is shown in Fig. 17(a). It is a planar version of the familiar waveguide oscillator with post-coupled varactor; it operates around 15 GHz and has comparable performance. The main advantage of the quasi-planar version, however, resides in the possibility of using nonpackaged varactor chips or beam-lead varactors with reduced parasitics.

Similarly, Cohen [13] placed a varactor half a wavelength from the Gunn device in the oscillator of Fig. 13(b) to achieve FM capability. This circuit is shown in Fig. 17(b).

Erichsen *et al.* [15 have reported a varactor-tuned oscillator circuit consisting of a 10 dB finline coupler of the branchline type, a Gunn diode connected to one of its ports, and two tuning varactors terminating the coupled ports (Fig. 18). Power is extracted either from the isolated port (a) or from the port with the active device (b). In the latter case, the isolated port must be terminated in a matched load. Tuning of the varactors controls the reflection coefficient seen by the Gunn diode. Frequency and output power can be adjusted independently by appropriate balance of the varactor bias voltages, thus eliminating all need for mechanical tuning. Output power levels between 10 and 20 mW in the 34 to 37 GHz range were obtained with both a DGB 8256 device from Alpha Industries and a TEO 44 device from Plessey.

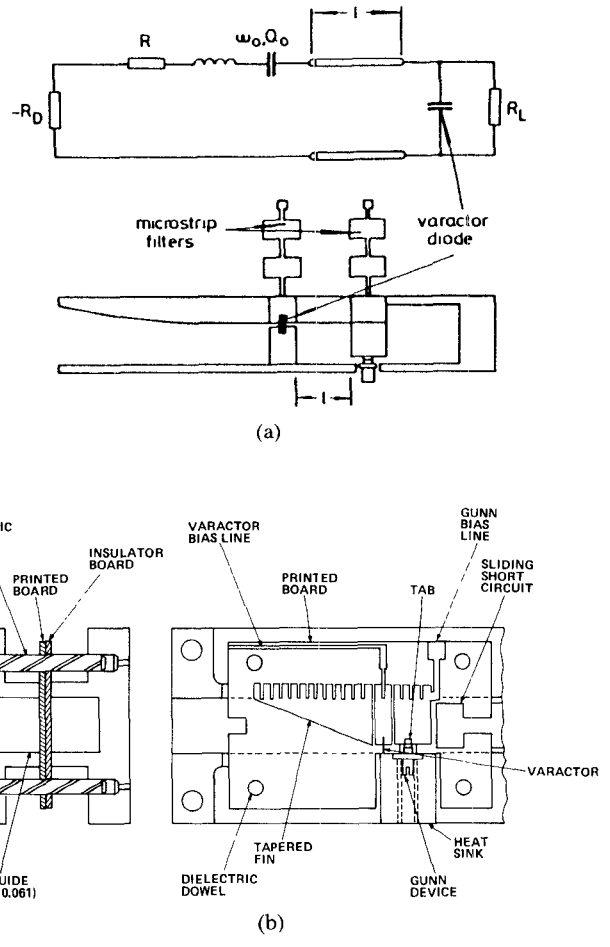

Fig. 17. Varactor-tuned planar Gunn oscillators. (a) Circuit by Knoechel [2]. (b) Circuit by Cohen [13].

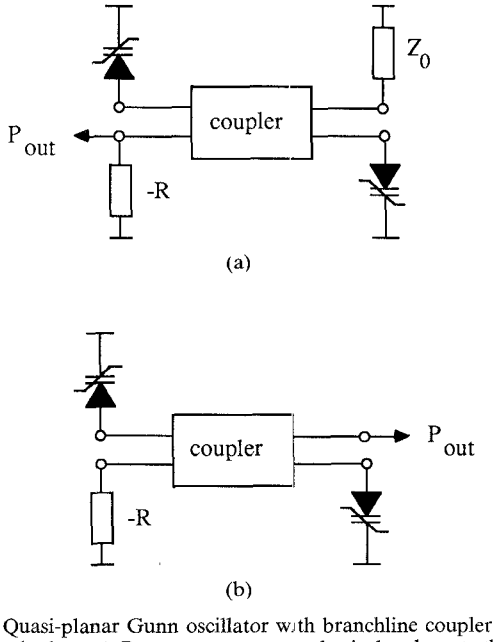

Fig. 18. Quasi-planar Gunn oscillator with branchline coupler and two varactor diodes. (a) Power extraction at the isolated port. (b) Power extraction at the device port. (After Erichsen, Schuenemann, and El Hennawy [15].)

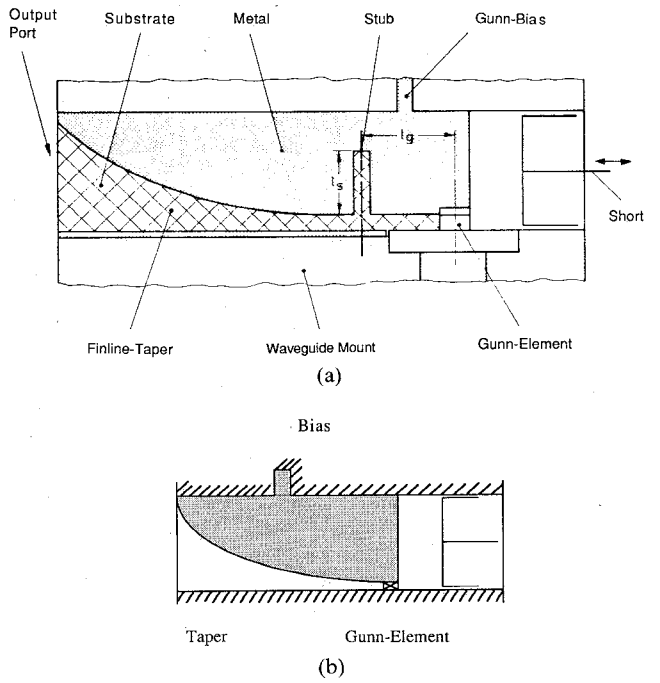

Fig. 19. Basic Gunn oscillators suitable for varactor tuning, by Solbach, Adelseck, and Sicking [16]. (a) 35 GHz oscillator. (b) 60 GHz oscillator.

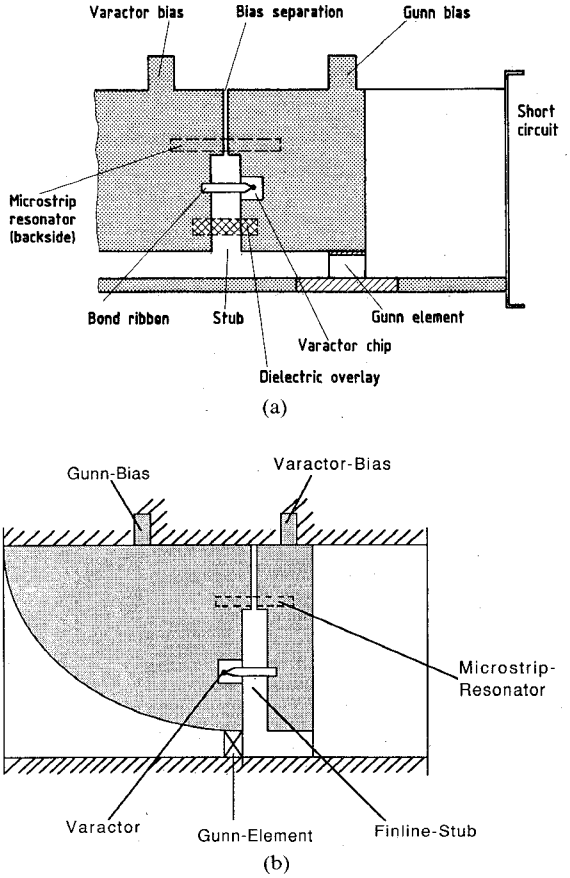

Fig. 20. Mounting of the varactor in the tuning slot. (a) 35 GHz Gunn oscillator. (b) 60 GHz Gunn oscillator. (After Solbach, Adelseck, and Sicking [16].)

Solbach *et al.* [16] have reported varactor-tuned oscillators for 35 and 60 GHz. The basic oscillator for 35 GHz is shown in Fig. 19(a). It is similar in design to the direct-mounted versions shown in Fig. 13, but contains a series stub for impedance matching. The series stub and the line between stub and diode form a $\lambda/2$ resonator, which is tapped at its center by the output line. The frequency of the oscillator can be tuned by varying the electrical length of this resonator with a varactor diode. This is accomplished with the arrangement shown in Fig. 20. In order to separate the bias networks for the Gunn element and the varactor, the front metallization is split along the axis of the stub. A microstrip resonator on the back of the substrate forms a short circuit at RF. The varactor is coupled to the slot via a 22-μm-wide bond ribbon; the inductance of the ribbon detunes the slot, and must thus be compensated by a small piece of dielectric material placed across the slot.

With this configuration, tuning ranges in excess of 1 GHz in *Ka*-band with power variations from 15 mW to 40 mW have been achieved using medium-power Gunn devices (MA 47172) [16]. Q factors of about 140 were measured.

In the 60 GHz oscillator (Fig. 20(b)), the tuning stub with the varactor is situated opposite to the load side, and its input impedance appears in series with the main slot, which ends in a short-circuited waveguide section. Since the tuning slot is nearly $\lambda/4$ long, the reactive load seen by the diode is very insensitive to the length of the waveguide section. For this arrangement, an output power of 20 mW at 63.7 GHz and a 400 MHz tuning range with power variations of less than 2 mW have been reported [16].

The bond ribbon used in the mounting of the chip varactor diode makes the reproduction of the tuning circuit difficult. The use of beam-lead varactors should considerably improve the reproducibility of the design.

III. IMPATT Diode Oscillators

In principle, the Gunn oscillator circuits described above can also accommodate IMPATT diodes. In practice, however, the design of *E*-plane IMPATT oscillators is extremely difficult because of the very low source impedance of the diodes and the sensitivity of their power output to the load impedance. Even if the large-signal parameters of a given diode were known accurately (they would have to be measured in a test oscillator) and an appropriate quasi-planar circuit had been designed for optimum power output, a similar device with slightly different characteristics would perform poorly in the same circuit. This is due to the large impedance ratio that must be overcome by the circuit. Since typical source impedances for IMPATT diodes in *Ka*-band are of the order of 8 Ω, the matching to a wave impedance of 200 Ω calls for a transformer ratio of 25. Even though such a ratio can be realized in quasi-planar technology, it is difficult to reproduce with accuracy, is very lossy, and the circuit, once printed, cannot be adjusted to compensate for the considerable variations in device parameters that occur from sample to sample. Inde-

pendent studies [14], [17] have led to the conclusion that the realization of IMPATT oscillators (and amplifiers) in E-plane technique is not very attractive. The reasons are essentially the same as those discussed for second-harmonic Gunn oscillators.

IV. Transistor Oscillators

Transistors are well suited for the realization of efficient and quiet oscillators for frequencies as high as 110 GHz. Both field effect transistors (FET's) and bipolar junction transistors (BJT's) have been used to build E-plane oscillators. Two approaches can be distinguished:

i) The transistor is directly embedded in the finline circuit.
ii) The transistor is embedded in a microstrip circuit which is mounted in the E plane of a waveguide. Power is extracted via an antipodal transition from microstrip to waveguide.

While the first approach facilitates integration of the oscillator into an E-plane circuit, the latter takes advantage of the compatibility of transistors with microstrip, and favors monolithic integration.

Passive stabilization of oscillators with dielectric resonators is practical up to 22 GHz. Beyond that frequency, second-harmonic extraction is preferable while the oscillator is stabilized at the first harmonic.

In the following, the properties of free-running oscillators with the transistor directly embedded in the finline environment will be described first. Then, DR stabilization techniques will be discussed, and the characteristics of stabilized fundamental and second-harmonic oscillators will be summarized. Finally, some realizations of microstrip FET oscillators with E-plane transitions will be mentioned.

A. Free-Running Finline Transistor Oscillators

The first finline FET oscillator was reported by Meinel [18]. The transistor is placed in the center of a series T junction in which two branches are terminated by variable shorts (see Fig. 21(a)). The three terminals of the device are connected with bond wires to three different fins, thus permitting dc isolation and separate biasing of the terminals.

The oscillator operates in the common-source mode. Its frequency is essentially determined by the length of the gate resonator, while the feedback, and hence the output power, are governed by the gate–drain resonator length. The transistor is matched to the output waveguide by a quarter-wave transformer, followed by a finline taper.

The variable backshorts are insulated with Teflon to minimize losses and wear of the finline circuit. They consist of three low-impedance and two high-impedance quarter-wave sections.

Both a packaged and an unpackaged device were tested at 30 GHz. While the packaged NE 388-06 device delivered only 0.38 mW with a dc-to-RF efficiency of 1.4 percent, the unpackaged sample from LEP achieved nearly 3 mW at 4 percent efficiency.

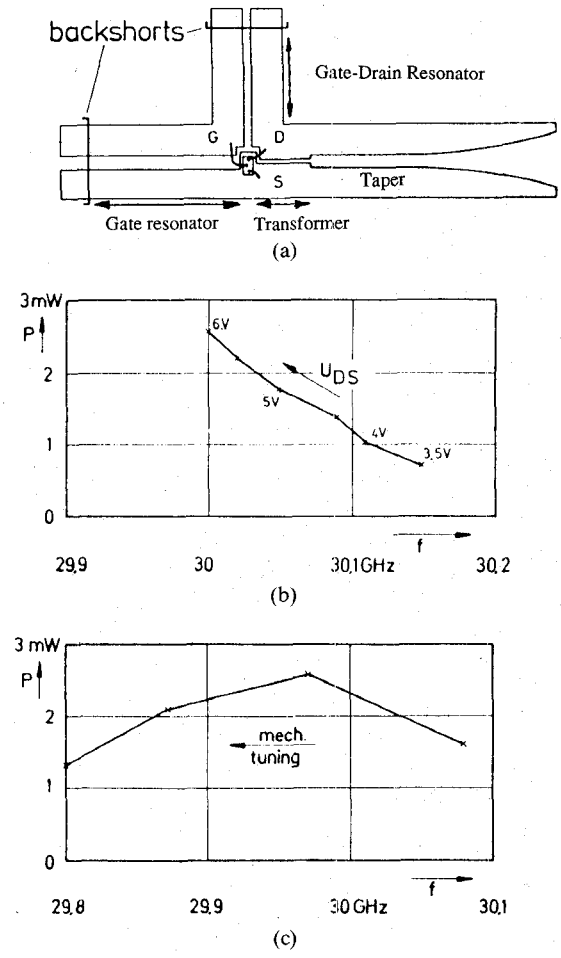

Fig. 21. 30 GHz finline FET oscillator. (a) Circuit layout. (b) Electrical tunability. (c) Mechanical tunability. (After Meinel [18].)

The oscillator could be tuned either mechanically (by changing the gate resonator length) or electrically (by varying the voltage between drain and source). Fig. 21(b) and (c) demonstrates the electrical and mechanical tunability of the oscillator containing the unpackaged device.

A different type of finline oscillator has been proposed by Jacob and Ansorge [19], [20]. It features a pair of boomerang-shaped slots which form a cross and are coupled to the gate and the drain of a transistor (see Fig. 22) placed in the center of the cross. Three of the finline branches are terminated with variable backshorts while the fourth, between drain and source, is connected to the output waveguide via a finline taper. In contrast to the Meinel oscillator, the gate and the drain do not share a common line section. Feedback must therefore be provided by means of a metal strip on the backside of the substrate. This feedback strip acts essentially as a half-wavelength microstrip resonator which is coupled magnetically to the slots, and therefore roughly determines the frequency of oscillation. Fine-tuning and maximum output power are achieved by adjusting the position of the shorts.

Various FET devices have been tested in such a circuit by Jacob and Ansorge. Fig. 23 shows the dc-to-ac conver-

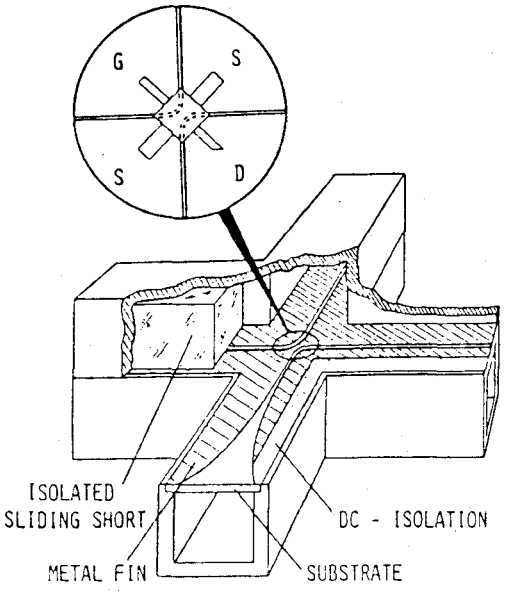

Fig. 22. Finline FET oscillator with separate gate and drain lines (after Jacob and Ansorge [19]).

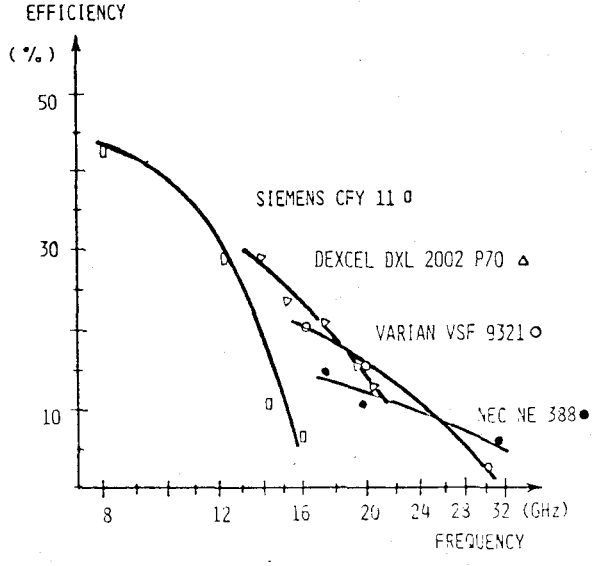

Fig. 23. Measured efficiencies of packaged FET's in a finline oscillator (after Jacob and Ansorge [19]).

sion efficiency of various packaged devices as a function of frequency. Using the circuit of Fig. 22, Ansorge [20] has obtained 7 dBm of output power with 10 percent efficiency at 13 GHz from an Avantek AT 41435 bipolar transistor, and observed that the phase noise was lower than that of a comparable FET oscillator.

Note that only in experimental oscillators are all backshorts variable. In a dedicated design, some or all of them may be replaced by fixed shorts. Special care must be taken to insulate the fins against the waveguide housing. This can be achieved either by inserting a thin Mylar or Teflon sheet between the fins and the enclosure or by interrupting the metallization by a narrow longitudinal slot along the waveguide walls, as indicated in Fig. 22.

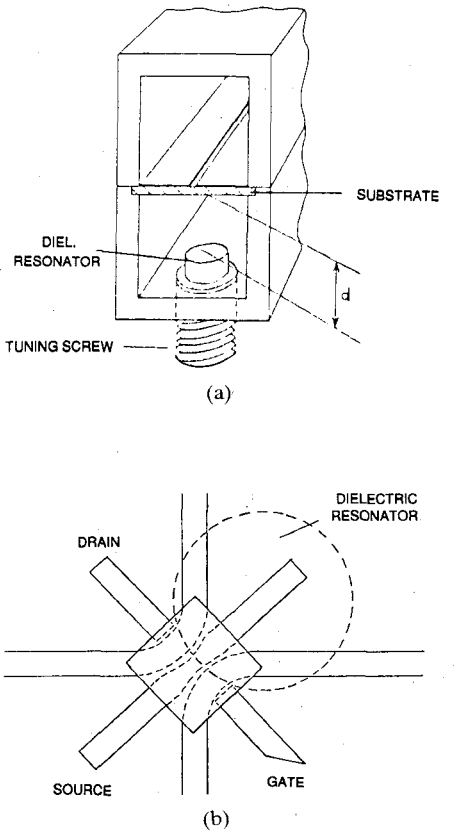

Fig. 24. Stabilization of finline FET oscillators with a dielectric resonator. (a) Adjustable mounting of a resonator in a finline (after Jacob and Ansorge [19]). (b) Mounting of a feedback resonator between gate and drain lines on the back side of the substrate. (after Gagnon, L'Ecuyer, and Hoefer [21]).

B. Transistor Oscillators Stabilized by a Dielectric Resonator

Three basic configurations are available for stabilizing an oscillator with a high-Q resonator. The resonator can be used as either a transmission, reaction, or feedback element. Jacob and Ansorge [19] have described a reaction-type oscillator, while Gagnon *et al.* [21] have realized feedback-type oscillators. The reaction resonator in the oscillator by Jacob and Ansorge is placed in one of the three usually short-circuited branches, which must then be terminated with a matched load, or in the output branch. Fig. 24(a) shows how the $TE_{01\delta}$ resonator is coupled with the finline. Both the resonant frequency and the coupling coefficient depend on the distance d between the resonator and the substrate. The main advantage of this arrangement is that it can be tuned mechanically from the outside of the housing. However, the thermal stability is not very high since the substrate is supported only at its borders and can therefore bend in an unpredictable way under the influence of thermal stress.

Gagnon *et al.* [21] therefore proposed to fix the dielectric resonator directly to the backside of the substrate such that it provided selective feedback between the drain and the gate lines, as shown in Fig. 24(b). Coupling to these

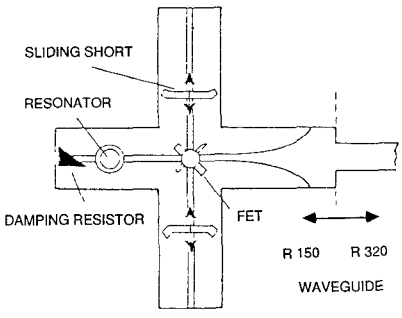

Fig. 25. Second-harmonic finline FET oscillator, stabilized by a dielectric resonator at the fundamental frequency (after Jacob and Ansorge [19]).

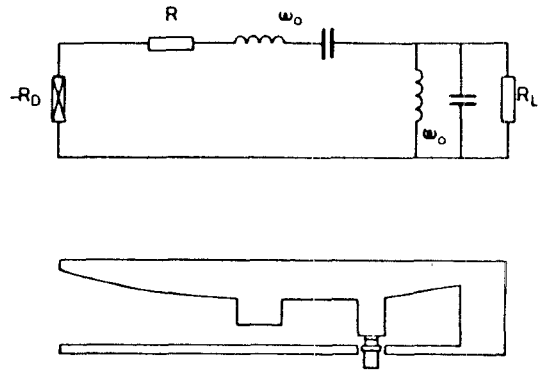

Fig. 26. *E*-Plane Gunn-diode oscillator with reactance compensation circuit (capacitive planar stub) for increased phase-locking range (after Knoechel [2]).

lines can be adjusted by moving the resonator along that diagonal axis of symmetry which does not intersect the lines. Using a NE 67383 (a low-noise MESFET with a recessed gate of 0.3 μm), 20 mW of power have been generated with such an oscillator at 24 GHz with an efficiency of 30 percent [21].

Note that even with a stabilizing resonator introducing additional losses, the efficiency of the oscillator can exceed 30 percent. Long-term thermal stability can be improved by choosing resonators with appropriate thermal coefficients and/or by using digital temperature control acting upon the transistor drain voltage. If extremely low phase noise is required, a high-Q transmission cavity resonating in the cylindrical TE_{01n} mode can be inserted in the output of the oscillator. For high temperature stability, such a cavity can be fabricated in titanium silicate and sealed to avoid frequency shift due to changes in atmospheric pressure and humidity [22].

C. Second-Harmonic Finline Transistor Oscillators

Second-harmonic extraction from finline oscillators has been reported by Jacob and Ansorge [19]. The oscillator has the same configuration as the fundamental oscillator shown in Fig. 22 with the exception of an abrupt change in waveguide size (R 150 to R 320) in the output, which reflects the energy at the fundamental frequency back into the oscillator while passing the second harmonic. By properly adjusting the position of the waveguide step and of the short in the gate line, an output power of 7 dBm at 31.4 GHz was achieved with an efficiency of 7 percent. The device used was a NE 38883 FET with a gate length of 0.5 μm. Second-harmonic extraction from an AT 41435 BJT yielded -5 dBm at 18.5 GHz with an efficiency of 2 percent [20].

Fig. 25 shows the same oscillator stabilized with a DR in the gate line. Since the fundamental frequency is practically not affected by the load at the second harmonic, the improvement in stability due to the DR is less dramatic than in fundamental oscillators. The factor of stabilization could be doubled at an expense of 0.4 dB in the output power.

It was also observed that the second-harmonic extraction oscillators had a relatively low noise level. This is due to the fact that the oscillator is terminated reactively at the fundamental frequency. With dielectric resonators being available for frequencies up to 22 GHz, DR-stabilized second-harmonic oscillators are feasible for frequencies up to 44 GHz.

D. Microstrip Transistor Oscillators with E-Plane Transition

The microstrip environment is, in general, more compatible with transistor technology than finline. It is therefore attractive to embed the device in a microstrip circuit followed by an E-plane transition to finline or waveguide. Such oscillators have been reported by Tserng and Kim [23], [24]. Using a 75×0.25 μm GaAs MESFET in a microstrip test fixture with an antipodal finline transition to waveguide, they have achieved 33 mW at 34 GHz with an efficiency of 30 percent, and similar output power at 40 GHz with an efficiency of 25 percent. A 75×0.2 μm GaAs FET was made to oscillate over the frequency range of 70 to 110 GHz in such a fixture. Power levels ranged from a few milliwatts in the 70 to 80 GHz range to about 0.1 mW at the maximum frequency of 110 GHz. The authors believe that up to 10 mW at 100 GHz could be achieved by optimizing the device and circuit implementation technique.

V. Amplifiers

Two types of E-plane amplifiers have been reported in the literature, namely the injection-locked type consisting essentially of a modified Gunn oscillator, and the transmission-type transistor amplifier with separate input and output matching networks.

A. Injection-Locked Gunn Diode Amplifiers

All Gunn oscillator types described above can, in principle, be injection locked and thus can be used as synchronous amplifiers. However, the locking range and gain may not be adequate for many purposes. To increase the locking range, the reactance compensation technique described in [25] may be used. This technique amounts to lowering the Q factor of the oscillator circuit by adding a so-called complementary resonant circuit. In the E-plane oscillator described by Knoechel [2] (see Fig. 26), this complementary circuit takes the form of a capacitive planar stub which, together with the line section separating it

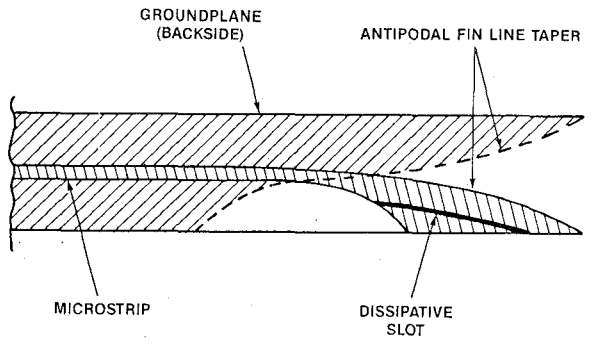

Fig. 27. Antipodal finline-to-microstrip transition with dissipative slot for mounting a transistor in a waveguide (after Ebner, Opfer, and Schweppe [26]).

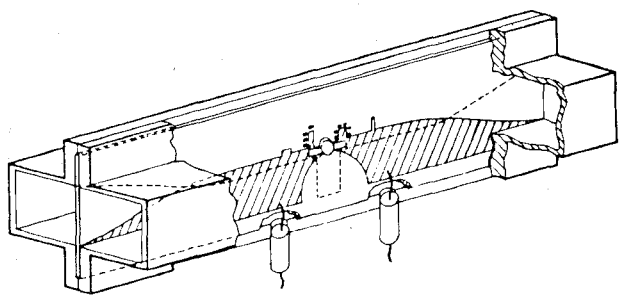

Fig. 28. *E*-plane FET amplifier by Derwischew and Senf [27].

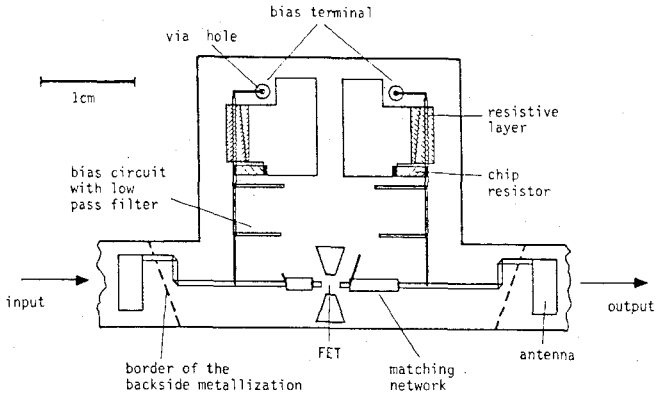

Fig. 29. Microstrip FET amplifier for insertion into a waveguide (after Meier, Hinken, and Stenzl [29]).

from the diode mount, forms a resonant loop. When the frequency of the locking signal deviates from the free-running frequency of the oscillator, one of the loops stores capacitive, and the other inductive energy, thus effectively broadening the locking range. By empirically adjusting the dimensions of the planar circuit, Knoechel [2] has obtained a relative locking bandwidth of 1.7 percent at 20 dB locking gain, and of 4.5 percent at 10 dB locking gain for a Gunn oscillator at 14.5 GHz. These values are similar to those obtained with waveguide oscillators.

B. Transistor Amplifiers

The realization of transistor amplifiers in quasi-planar technology is more problematic than that of oscillators. The main reason for this resides in the difficulty of achieving unconditional stability in the quasi-planar waveguide environment. The distributed nature of the fields makes it difficult to suppress unwanted feedback, and the cutoff behavior of the lines causes purely reactive source and load impedances at low frequencies.

To overcome this difficulty, most researchers [26]–[31] have realized the amplifier core, i.e., the transistor with its input and output matching networks, in microstrip and then provided appropriate transitions to waveguide, thus effectively realizing an *E*-plane component.

1) Microstrip Transistor Amplifiers with E-Plane Transitions: Ebner *et al.* [26] have described a microstrip transistor mount with antipodal finline-to-microstrip transitions (Fig. 27). To stabilize the device at frequencies below cutoff, they have added a dissipative slot. Even though a very good RF-to-dc isolation can be achieved in this manner, the addition of absorbing material and of long lossy transitions is detrimental to the performance of an amplifier realized in this fashion.

An amplifier with similar features for 9.2 GHz has been reported by Derwischew and Senf [27] (Fig. 28). A packaged GAT 6 GaAs FET from Plessey is mounted in a short microstrip section between two antipodal finline transitions. The matching networks are realized in the antipodal environment, and bias is applied via the fins, thus eliminating the need for a low pass in the bias network. A gain of 9 dB with a noise factor of 4 dB has been measured at 9.2 GHz. The concept can be extended to much higher frequencies: Berenz *et al.* [28] have reported a 60 GHz amplifier using a 0.25-μm-gate-length depletion-mode HEMT in the same type of circuit, realized on quartz substrate. A gain of 7.5 dB has been achieved at 60 GHz in a single stage.

Meier *et al.* [29] have realized a microstrip amplifier suitable for insertion into a waveguide (Fig. 29). Again, the RF matching and the bias circuits required for unconditional stability are fabricated in microstrip. However, the transition to waveguide is realized in the form of a printed antenna. Each transition and its connecting microstrip line add about 0.5 dB of insertion loss to the amplifier. With a Mitsubishi MGF 1303 GaAs FET, the amplifier achieved an overall gain of 9 ± 1.3 dB over a bandwidth of 3.3 GHz centered at 10.4 GHz, and a noise figure of less than 3 dB.

The amplifier described by Ruxton *et al.* [30], [31] employs a different kind of transition between the microstrip and the finline/waveguide environment. The input and output lines of the microstrip amplifier are each terminated in a bandstop filter. (See [31, fig. 1], this issue.) This filter presents an open circuit at $\lambda/4$ (at the center frequency of the amplifier) from a microstrip-to-finline transition, but is transparent at all other frequencies, thus presenting a 50 Ω bias resistance to the transistor outside the stopband. With a NEC NE67300 device, this amplifier delivers a stable overall gain of 6 dB at 20 GHz and has a 3 dB bandwidth of 3.6 GHz and a noise figure of less than 4 dB.

2) Finline Transistor Amplifier: The only amplifier in which the transistor is directly embedded in the finline

environment is that proposed by L'Ecuyer *et al.* [32], [33]. This design was inspired by the oscillator configuration given by Jacob and Ansorge [19]. But in contrast to the former, the input and output finlines run straight and in parallel rather than in a boomerang shape. In addition, they are shielded from each other by a thin electric wall or septum; this transforms the slots on either side into single-fin lines, which have only half the impedance of a regular symmetrical finline. The transistor chip sits in a narrow opening of the septum, and is coupled magnetically to the input and output lines with bond wires, as shown in [33, fig. 1(b)] (this issue). The source pads of the FET chip are grounded to the central metallization. For maximum magnetic coupling, the finlines are short-circuited at about one quarter wavelength beyond the bond wires. Fine matching of the input and output impedances of the FET is achieved by adjusting the length of a shunt tuning slot in each line with silver paint.

The circuit is printed on 0.010-in.-thick RT/Duroid ($\epsilon_r = 2.22$). In order to prevent any RF coupling between the input and output lines through the substrate, a series of plated-through holes runs along the line of separation, thus extending the shielding septum into the dielectric. By keeping the distance between holes much smaller than the wavelength in the substrate, one can (in the absence of the transistor) reduce the coupling between input and output to less than -30 dB.

Special gate and drain bias circuits overcome the problem of instability at frequencies below finline cutoff. At RF, the bias circuits are invisible to the transistor while presenting a good match at lower frequencies, where the finline becomes reactive. They consist of a $\lambda/2$ coplanar section and a microstrip filter which reduces RF leakage into the bias circuit.

Using a NE67300 FET, unconditionally stable operation with more than 6 dB amplification over a 1 GHz bandwidth centered at 16.8 GHz could be achieved. The measured noise figure was 3.5 dB.

VI. Discussion and Conclusion

A variety of oscillators and amplifiers in E-plane technology have been described, and their most important design features and performance characteristics have been summarized. Note that the tapered transitions to waveguide, which can be seen in almost all figures, are provided for interfacing the components with waveguide instrumentation. They are superfluous whenever the component is to be integrated with other E-plane structures, as in Fig. 1.

It appears that transistors provide very efficient signal generation for frequencies up to 110 GHz. By virtue of the very low parasitic emitter inductance in the quasi-planar mounting, even bipolar transistors provide power up to 18 GHz using second-harmonic extraction at very low cost and with excellent phase noise. FET's are well suited for realizing local oscillators with power levels sufficient for most applications. For fundamental frequencies below 22 GHz, they can easily be stabilized with dielectric resonators.

E-plane Gunn diode oscillators generate frequencies up to 100 GHz. Being less sensitive to variations in the load impedance than IMPATT diodes, they perform well in an E-plane circuit. The performance of such oscillators rivals that of waveguide oscillators if the slot width approaches the enclosure height. Circuit Q factors decrease with decreasing slot width and increasing number of circuit tuning elements, as exemplified by the resonator-mounted and grating oscillators. Electronic frequency tuning is easily accomplished with beam-lead varactors, which are highly compatible with quasi-planar technology. Most oscillators can be injection-locked; a technique for broadening the locking range has been indicated.

IMPATT oscillators and second-harmonic Gunn oscillators are not well suited for E-plane realization. The main obstacle is the large impedance transformer ratio that must be overcome by the planar circuit. The resulting requirements exceed the capabilities of present design tools, and the printed circuits are not amenable to the critically fine adjustments needed for optimizing such oscillators.

E-plane transistor amplifiers have been built for frequencies up to 60 GHz using MESFET and HEMT devices. With one exception, the transistor is embedded in a microstrip environment, and appropriate input and output transitions are provided. Unconditional stability is obtained in all cases by careful design of the bias circuitry.

HEMT devices have not yet been directly embedded in a finline environment, and there is room for further development of frequency multipliers, dividers, active mixers, and similar components exploiting the circuit configurations discussed above. Furthermore, much work remains to be done on the modeling of passive structures employed in the realization of active components. The general availability of such models in a form suitable for CAD would greatly facilitate routine design of E-plane components and enhance the attractiveness of this technology for millimeter-wave applications.

References

[1] R. P. Owens and D. Cawsey, "Microwave equivalent-circuit parameters of Gunn-effect-device packages," *IEEE Trans. Microwave Theory Tech.*, vol. MTT-18, pp. 790–798, Nov. 1970.

[2] R. Knoechel, "Design and performance of microwave oscillators in integrated fin-line technique," *Microwave, Optics, Acoust.*, vol. 3, no. 3, pp. 115–120, May 1979.

[3] H. El Hennawy and K. Schuenemann, "Computer-aided design of active fin-line circuits," in *12th European Microwave Conf. Dig.* (Helsinki, Finland), 1982, pp. 691–696.

[4] Q. Zhang and T. Itoh, "Spectral-domain analysis of scattering from E-plane circuit elements," *IEEE Trans. Microwave Theory Tech.*, vol. MTT-35, pp. 138–150, Feb. 1987.

[5] G. Begemann, E. Kpodzo, and A. Schlegel, "A *Ku*-band fin-line front-end with a hybrid-coupled balanced mixer and a Gunn oscillator," in *10th European Microwave Conf. Dig.* (Warszawa, Poland), 1980, pp. 750–753.

[6] H. Hofmann, H. Meinel, and B. Adelseck, "New integrated mm-wave components using fin-lines," in *1978 IEEE MTT-S Int. Microwave Symp. Dig.* (Ottawa, Canada), pp. 21–23.

[7] E. Pic and W. J. R. Hoefer, "Experimental characterization of fin line discontinuities using resonant techniques," in *1981 IEEE MTT-S Int. Microwave Symp. Dig.* (Los Angeles, CA), pp. 108–110.

[8] H. Hofmann, "MM-wave Gunn oscillator with distributed feedback fin-line circuit," in *1980 IEEE MTT-S Int. Microwave Symp. Dig.* (San Diego, CA), pp. 59–61.

[9] T. Itoh and F.-J. Hsu, "Distributed Bragg reflector Gunn oscillators for dielectric millimeter-wave integrated circuits," *IEEE Trans. Microwave Theory Tech.*, vol. MTT-27, pp. 514–518, May 1979.
[10] M. Burton and W. J. R. Hoefer, "An improved model for short- and open-circuited series stubs in fin lines," in *1984 IEEE MTT-S Int. Microwave Symp. Dig.* (San Francisco), pp. 330–332.
[11] B. Adelseck, F. Sicking, and H. Hofmann, "Gunn-Oscillatoren mit periodisch belasteten Finleitungen," *Wiss. Ber. AEG-Telefunken*, vol. 54, nos. 4–5, pp. 235–237, 1981.
[12] L. D. Cohen and P. Meier, "Advances in *E*-plane printed millimeter-wave circuits," in *1978 IEEE MTT-S Int. Microwave Symp. Dig.* (Ottawa, Canada), pp. 27–29.
[13] L. D. Cohen, "Advances in printed mm-wave oscillator circuits," in *1980 IEEE MTT-S Int. Microwave Symp. Dig.*, (Washington, DC), pp. 264–266.
[14] AEG AG, Ulm, West-Germany, private communication.
[15] K. Erichsen, K. Schuenemann, and H. El Hennawy, "MM-wave fin-line oscillator with electronic matching and tuning," in *12th European Microwave Conf. Dig.* (Helsinki, Finland), 1982, pp. 687–690.
[16] K. Solbach, B. Adelseck, and F. Sicking, "Finline varactor-tuned Gunn-oscillators for 35 and 60 GHz," *Mikrowellen Magazin* (Military Electronics), vol. 9, no. 1, pp. 64–66, 1983.
[17] M. Burton, "The IMPATT amplifier in fin line," M.A.Sc. thesis, University of Ottawa, Ottawa, Canada, June 1985.
[18] H. Meinel, "A 30 GHz FET oscillator using fin line circuitry," in *11th European Microwave Conf. Dig.* (Amsterdam), Sept. 1981, pp. 297–300.
[19] A. Jacob and C. Ansorge, "Stabilized fin-line FET oscillators," in *13th European Microwave Conf. Dig.* (Nuernberg), Sept. 1983, pp. 303–307.
[20] C. Ansorge, "Bipolar transistor *Ku*-band oscillators with low phase noise," in *1986 IEEE MTT-S Int. Microwave Symp. Dig.* Baltimore, MD), pp. 91–94.
[21] A. Gagnon, J. L'Ecuyer, and W. J. R. Hoefer, "An integrated millimeter-wave receiver frontend in *E*-plane configuration," in *IEEE Electronicom'85 Dig.* (Toronto), 1985, pp. 582–585.
[22] G. Painchaud, D. S. James, and W. J. R. Hoefer, "Aperture coupling between microstrip and resonant cavities," *IEEE Trans. Microwave Theory Tech.*, vol. MTT-25, pp. 392–398, May 1977.
[23] H. Q. Tserng and B. Kim, "*Q*-band GaAs MESFET oscillator with 30% efficiency," *Electron. Lett.*, vol. 24, no. 2, pp. 83–84, 21st Jan. 1988.
[24] H. Q. Tserng and B. Kim, "110 GHz GaAs FET oscillator," *Electron. Lett.*, vol. 21, no. 5, pp. 178–179, 28th Feb. 1985.
[25] R. Knoechel and K. Schuenemann, "Reactance compensation techniques for injection locked amplifiers," *Arch. Elek. Übertragung.*, vol. 33, pp. 49–56, 1979.
[26] H. Ebner, J. Opfer, and E. G. Schweppe, "A new integrated waveguide transistor mount," in *13th European Microwave Conf. Dig.*, (Nuernberg), Sept. 1983, pp. 266–271.
[27] S. Derwischew and W. Senf, "An *X*-band fin-line receiver," in *8th Colloq. Microwave Commun. Dig.* (Budapest), Aug. 1986, pp. 81–82.
[28] J. Berenz, K. Nakano, Ting-ih Hsu, and J. Goel, "HEMT 60 GHz amplifier," *Electron. Lett.*, vol. 21, no. 22, pp. 1028–1029, 24th Oct. 1985.
[29] U. Meyer, J. H. Hinken, and W. Stenzl, "A broadband FET amplifier in integrated waveguide technology with an *E*-plane microstrip insert," in *17th European Microwave Conf., Dig.* (Rome), Sept. 1987, pp. 119–124.
[30] J. Ruxton, R. Vahldieck, and W. J. R. Hoefer, "A 20 GHz FET amplifier in an integrated finline "microstrip" configuration," in *1988 IEEE MTT-S Int. Microwave Symp. Dig.* (New York), pp. 769–772.
[31] J. Ruxton and W. J. R. Hoefer, "A quasi-planar FET amplifier in integrated finline and microstrip technique," pp. 429–432, this issue.
[32] J. L'Ecuyer, G. B. Gajda, and W. J. R. Hoefer, "A FET amplifier in fin-line technique," in *1986 IEEE MTT-S Int. Microwave Symp. Dig.* (Baltimore), pp. 287–290.
[33] J. L'Ecuyer, G. B. Gajda, and W. J. R. Hoefer, "A FET amplifier in finline technique," pp. 425–428, this issue.

✠

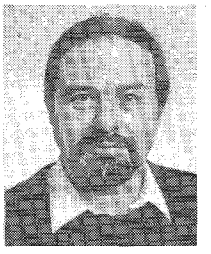

Wolfgang J. R. Hoefer (M'71–SM'78) received the diploma in electrical engineering from the Technische Hochschule Aachen, Aachen, Germany, in 1964, and the D. Ing. degree from the University of Grenoble, Grenoble, France, in 1968.

After one year of teaching and research at the Institut Universitaire de Technologie, Grenoble, France, he joined the Department of Electrical Engineering, University of Ottawa, Ottawa, Ont., Canada, where he is currently a Professor. His sabbatical activities have included six months with the Space Division of the AEG-Telefunken in Backnang, Germany, six months with the Electromagnetics Laboratory of the Institut National Polytechnique de Grenoble, France, and one year with the Space Electronics Directorate of the Communications Research Centre in Ottawa, Canada. His research interests include microwave measurement techniques, millimeter-wave circuit design, and numerical techniques for solving electromagnetic problems.

Dr. Hoefer is a registered Professional Engineer in the province of Ontario, Canada.